

## Determination of optimum filter in myocardial SPECT: A phantom study

A. Takavar<sup>1\*</sup>, Gh. Shamsipour<sup>1</sup>, M. Sohrabi<sup>2</sup>, M. Eftekhari<sup>2</sup>

<sup>1</sup>Department of Medical Physics, Tehran University of Medical Sciences, Tehran, Iran

<sup>2</sup>Research Institute for Nuclear Medicine, Shariati Hospital, Tehran University of Medical Sciences, Tehran, Iran

---

### ABSTRACT

**Background:** In myocardial perfusion SPECT imaging, images are degraded by photon attenuation, the distance-dependent collimator, detector response and photons scatter. Filters greatly affect quality of nuclear medicine images

**Materials and Methods:** A phantom simulating heart left ventricle was built. About 1mCi of <sup>99m</sup>Tc was injected into the phantom. Images were taken from this phantom. Some filters including Parzen, Hamming, Hanning, Butterworth and Gaussian were exerted on the phantom images. By defining some criteria such as contrast, signal to noise ratio, and defect size detectability, the best filter can be determined.

**Results:** 0.325 Nyquist frequency and 0.5 Nq was obtained as the optimum cut off frequencies respectively for hamming and hanning filters. Order 11, cut off 0.45 Nq and order 20 cut off 0.5 Nq obtained optimum respectively for Butterworth and Gaussian filters.

**Conclusion:** The optimum member of every filter's family was obtained. *Iran. J. Radiat. Res., 2004; 1(4): 205-210*

---

**Keywords:** SPECT, phantom, filter.

### INTRODUCTION

The degrading factors are exacerbated in patients with large sub-diaphragmatic uptake, and in patients with large breasts, noise also degrades the images, and image texture is affected by filter parameters, reconstruction algorithm and compensation method (Sankaran *et al.* 2002).

Parameters determining the choice of the SPECT filter type are:

1. The number of counts (limited by patient radiation burden and by increased movement artifacts related to study time).
2. The type of study (organ)
3. The background noise level
4. The personal choice of the interpreting physician (Van Laere *et al.* 2002)

---

\* Corresponding author:

Dr. A. Takavar, Dept. of Medical Physics, Tehran University of Medical Sciences, Tehran, Iran.

E-mail: [Takavar@sina.tums.ac.ir](mailto:Takavar@sina.tums.ac.ir)

### MATERIALS AND METHODS

#### A. Phantom

The numbers of counts in the organ strongly affect the choice of a filter. Since the counts level in patients vary in each patient, we decided to find the effect of our filters on a constant input (with the same count for all filters). Right wall of heart has less uptake and can not be seen in myocardial SPECT.

Therefore we built a phantom simulating the left ventricle including septum and left wall. The phantom was made from Plexiglas and consists of two concentric cylinders with a half-spherical end cup on each end. Inner cylinder forms the ventricular chamber with 8 cm length and 4 cm diameter. The space between the two cylinders forms the myocardial wall chamber of 1 cm thickness (figure 1).

A defect also made of Plexiglas with 1 cm thickness was inserted in the chamber to indicate cold defect.

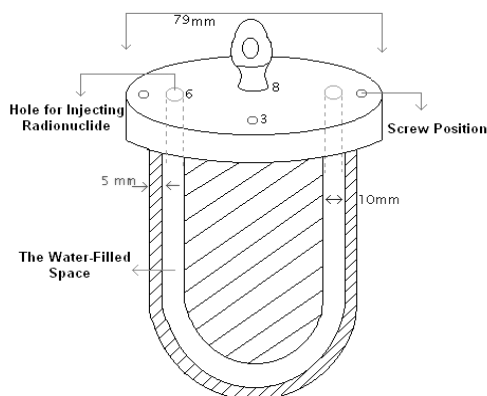


**Figure 1.** Schematic shape of cardiac phantom.

In our experiment, the myocardial wall chamber was filled with 1 mCi of  $^{99m}\text{Tc}$  sestamibi solution (Liang *et al.* 1998).

Some balloons were filled and 1 mCi Tc solution (as a background noise) were located in body phantom. The cardiac phantom was inserted in these balloons so that the heart phantom has the alignment like normal heart in the chest.

In clinical practice about 20 mCi of  $^{99m}\text{Tc}$  is injected into patient from which about 1 mCi is taken by myocardium.

### B. Acquisition

Imaging was performed using a double-head ADAC ,SOLUS model SPECT camera and in the nuclear medicine department of shariati hospital.

A low energy general-purpose collimator was used for imaging. Images were recorded over  $180^\circ$  from  $45^\circ$  right anterior oblique to  $45^\circ$  left posterior oblique in  $64 \times 64$  matrices with an acquisition time of 25 seconds per projection and 32 projections.

### C. Phantom quantitative analysis

To find the optimum filter, we used some criteria including contrast, SNR (signal to noise ratio) and defect size.

#### Contrast

We draw some regions of interest (ROI) on a vertical long axis view of our phantom. Our camera software provides us with information including total counts, mean

count, maximum & minimum count and number of counts in any ROI.

To obtain the maximum contrast of defect detection, we used the following formula

$$\text{MaxContrast} = \frac{\text{Maxcount(Norm)} - \text{Mincount(Def)}}{\text{Maxcount(Norm)}}$$

In this expression, *Norm* refers to normal myocardium and *Def* to defect. We obtained the difference of maximum count in normal myocardium from the minimum count in defect region. Later on we divided this difference to maximum count in (*Norm*).

#### SNR

To obtain SNR of defect diagnosis, the difference of maximum count in normal region from minimum count in the defect region was divided to minimum count in background (heart hole region) as follow:

$$\text{SNR} = \frac{\text{Maxcount(Norm)} - \text{Mincount(Def)}}{\text{Mincount(Background)}}$$

#### Defect Size

Some authors have dealt with determination of defect size (Matsunari *et al.* 2001).

To find filter that shows the defect size better, a line profile was drawn on the defect.

As is referred in reference (Beekman *et al.* 2001), the peaks at the two sides of the defect are not equal because of the different attenuation.

Since the software attached discrete points to each other, we decided to fit a two Gaussian function on our data, which were obtained from the line profile:

$$Y = \#A \cdot \exp(-0.5 * ((X - \#B) / \#C)^2) \\ + \exp(-0.5 * ((X - \#B) / \#C)^2) \\ + \#D \cdot \exp(-0.5 * ((X - \#E) / \#F)^2)$$

The fitting was done by "Table Curve" software- a good choice for curve fitting. The coefficients after # were determined by the software. This software, also gave us information like percent of confidence, the coefficients of the best-fitted equation, and the coordinates of every point that cursor was placed on.

It was observed that the width of the valley between two peaks varies with changing of the filter. We measured the distance between the smaller peak and the steep of the other peak having same count. We could move cursor and find the distance between two points (figure 2).

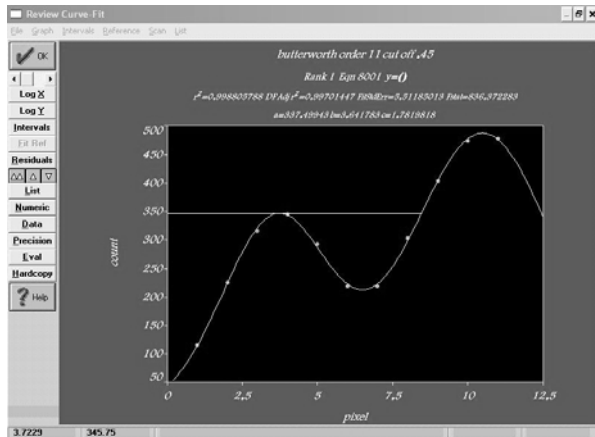


Figure 2. The fitted curve by software and the information provided by it.

### Final Criterion

We allocated a mark to every filter's contrast and SNR, a number from 1 to 20; 1 for the worst and 20 for the best case. Because the Butterworth and Gaussian filters have so many choices we preferred to assign marks from 1 to 100.

Our defect size was 1 cm and all filters showed the defect with larger size. So we gave

mark 1 for the largest number and 20 (or 100) for smallest one.

Finally we added all marks and obtained the overall points for each case, and comparison was made afterward.

## RESULTS

### Parzen

Parzen filter was visually excluded from our study because we could not even see the heart hole properly.

### Hamming

The generalized hamming filter was defined as below:

$$f(\omega) = \begin{cases} \alpha|\omega| + (1-\alpha)|\omega| \cos(\pi\omega/\Omega) & |\omega| < \Omega \\ 0 & |\omega| \geq \Omega \end{cases}$$

In this expression  $\Omega$  is critical frequency,  $\alpha$  is parameter in the range  $0 \leq \alpha \leq 1$  (Kramer and Sanger 1995). We selected the cut-off frequency of this filter from 0.3 to 0.5 with steps equal to 0.05.

According to our results the cut-off frequencies of 0.3 Nyquist frequency provided optimum defect size, 0.325 Nq indicated the best contrast and 0.5Nq offered the best SNR. The cut off frequency of 0.325Nq gave the best overall result (table 1 and figure 3).

Table 1. The results of Hamming filter.

Hamming Filter									
Cut off frequency ( $\times 0.5$ nyquist)	1	0.95	9	0.85	0.8	0.75	0.7	0.65	0.6
defect size	4.51	4.51	4.49	4.47	4.37	4.14	4.09	3.87	3.6
contrast	0.63	0.61	0.62	0.65	0.54	0.54	0.57	0.7	0.46
Snr	3.2	3.03	2.81	2.99	2.3	2.32	1.72	2.56	1.53
df/20	1	1	1.42	1.84	3.92	8.73	9.77	14.36	20
cnt/20	14.64	12.98	13.54	16.29	6.91	7.23	9.59	20	1
snr/20	20	18.14	15.57	17.67	9.78	9.95	3.1	12.69	1
total	35.64	32.12	30.52	35.8	20.62	25.91	22.46	47.05	22
Total (from 20)	11.88	10.71	10.17	11.93	6.87	8.64	7.49	15.68	7.33

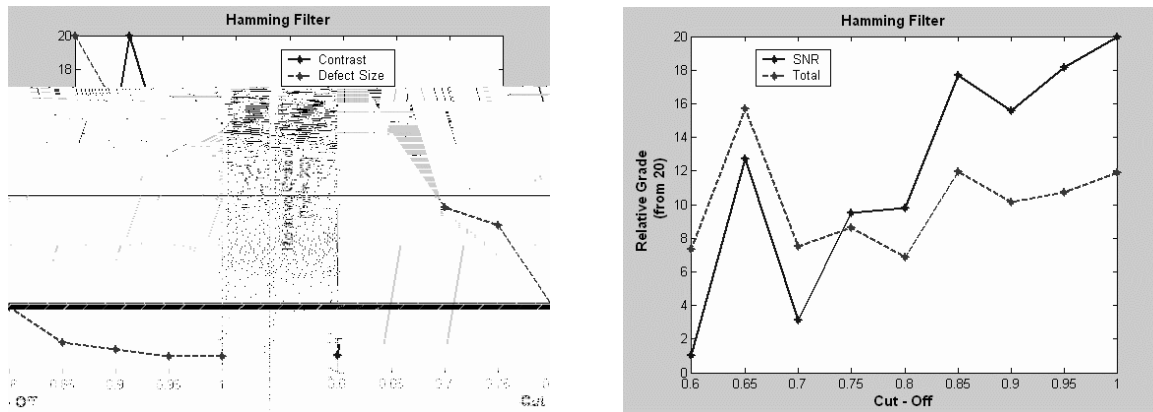


**Figure 3.** The contrast, SNR, defect size, and total results for hamming filter.

### Hanning

The Hanning filter was defined in the frequency domain as :

$$H(\nu) = \begin{cases} 0.5 + 0.5 \cos(\pi \nu / \nu_c) & 0 \leq \nu \leq \nu_c \\ 0 & \text{otherwise} \end{cases}$$

The cut-off frequency,  $\nu_c$ , determined when the function reached zero gain (David *et al.* 1988). This filter also had one variable parameter (cut-off

frequency). For this filter the cut off frequencies were selected from 0.3 to 0.5 with 0.05 step, like hamming. According to our results the cut-off frequencies of 0.3 Nyquist frequency provided optimum defect size, 0.5 Nq indicated the best contrast and .0.45Nq offered the best SNR. The cut off frequency of 0.5 Nq gave the best overall result. Table 2 and figure 4 show the results of hanning filter.

**Table 2.** The results of Hanning filter.

Hanning Filter									
Cut off frequency ( $\times 0.5$ nyquist)	1.00	0.95	0.90	0.85	0.80	0.75	0.70	0.65	0.60
defect size	4.48	4.45	4.44	4.37	4.24	4.07	3.92	3.73	3.32
contrast	0.63	0.60	0.59	0.58	0.59	0.54	0.57	0.55	0.49
Snr	2.74	2.86	2.92	2.77	2.44	2.00	1.84	1.66	1.46
df/20	1.00	1.49	1.66	2.80	4.93	7.72	10.17	13.28	20.00
cnt/20	20.00	16.37	14.69	12.74	14.69	7.85	11.76	9.24	1.00
snr/20	17.63	19.30	20.00	18.09	13.72	8.07	5.98	3.65	1.00
Total (from 20)	12.88	12.54	12.12	11.21	11.12	7.88	9.30	8.73	7.33

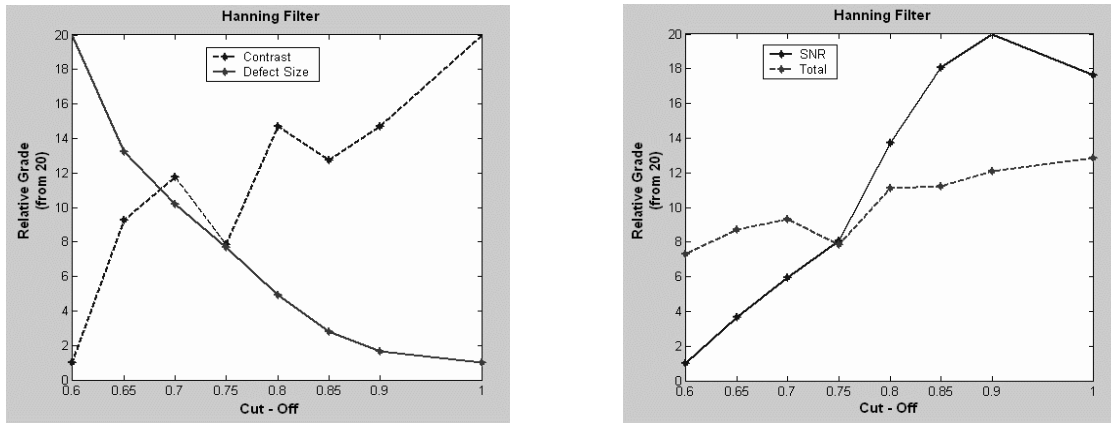


Figure 4. The contrast, SNR, defect size, and total results for hanning filter.

### Butterworth

A butterworth filter in the frequency domain (f) was shaped like a curve, which is described by the following equation:

$$\text{Butterworth} = \frac{1}{1 + \left(\frac{f}{f_c}\right)^{2n}}$$

$f_c$  is the cut-off frequency and  $n$  is the order of the filter (Germano 2001).

This formula has two variable parameters i.e. cut off frequency and order. In Shariati nuclear medicine center, cut off frequency of 0.45 Nq and order of 11 were routinely used as optimum parameters.

We started cut -off frequencies from 0.3 to 0.8 with step of 0.1 and order from 3 to 12.

It was found that the cut-off frequencies of 0.3 Nyquist frequency and order 8 provided optimum defect size, 0.6 Nq and order 8 indicated the best contrast and 0.45Nq and order 11 offered the best SNR. The cut off frequency of 0.45 Nq and an order 11 gave the best overall result (figure 5).

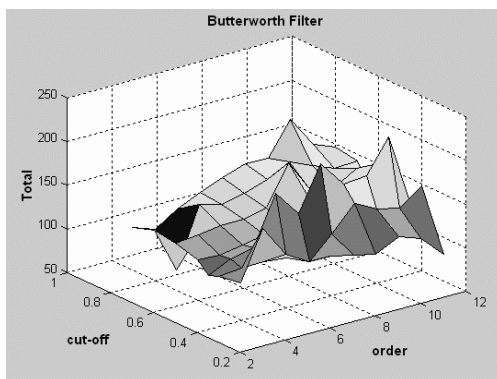


Figure 5. The final result of Butterworth filter.

### Gaussian

Gaussian function can be specified in two dimensions as

$$f(u) = e^{-\frac{(u-u_0)^2}{2\delta^2}} \quad u \geq 0$$

Where  $u$  is spatial frequency,  $u_0$  is the displacement of the gaussian from the origin and  $\delta$  specifies the spread (Madsen and Park 1985).

Although Michael A. King and his colleague have discussed Metz and Wiener filter and mentioned advantages of them (King and Schwinger 1984), the disadvantages of these filters have been discussed by Madsen and Park (1985).

This formula also has two variables parameter i.e. cut off frequency and order. The order 10 to 22 with step 2; and, cut-off 0.2 to 0.8 with step 0.1 were chosen for comparison.

Some of them were visually rejected.

Order 10 and cut-off 0.5Nq had best defect size. Order 20 and cut-off 0.6 Nq showed the best contrast. Order 22 and cut-off 0.4 Nq gave the best SNR.

As a whole order 20 and cut-off 0.5Nq provided best choice of this filter.

## DISCUSSION

We evaluated the contrast between defect and the normal in phantom. When the cut off frequencies of hamming and hanning filters were low, the high frequencies were not amplified. Since the high frequencies were related to defect region, so low cut off frequencies amplifies most

normal regions rather than the defected regions. Variations of contrast with cut off frequencies were seen in contrast diagrams.

In defect size diagrams it could be seen that the size of defect was reduced by reduction in cut off frequencies. Low cut off frequencies behaved as Ramp filter, therefore better resolution could be obtained in this case.

In SNR diagrams since noise corresponded to high frequencies, so the filters with different cut off frequencies showed different SNR. In both hamming and hanning filters the SNR improved with increasing the cut off frequencies. The final point that should be considered is that the overall diagrams of Gaussian and Butterworth filters show that one can not see a single unique peak in these diagrams. Therefore further study should include final observation of the patient by physician.

Many authors have dealt with filter in their studies. Although most of them have proposed Metz and Wiener as filter of choice, the disadvantages of these filters had been discussed - knowing the MTF and noise level of the system (King and Schwinger 1984). Van Laere (Van laere *et al.* 2002) has suggested the use of Butterworth as the best choice between filters. Since the final interpreter of images are medics, therefore our phantom results must be compared with those SPECT images obtained from patients.

## REFERENCES

- Beekman F. J., Kamphais C., King M. A., Van Rijk P. P. (2001). Improvement of image resolution & quantitative accuracy in clinical SPECT. *Computerized Medical Imaging and Graphics*, **25**: 135-146.
- David R.G., Tsui B. M., MC Cartney W.H., Perry J. R. (1988). Determination of the optimum filter function for SPECT imaging. *Journal of Nuclear Medicine*, **29**: 643-650.
- Germano G. (2001). Technical aspects of myocardial SPECT imaging. *Journal of Nuclear Medicine*, **42**: 1499-1507.
- Liang Z., Ye J., Cheng J., Li J. (1998). Quantitative cardiac SPECT in 3 dimensions validation by experimental photon studies. *Phys. Med. Biol.*, **43**: 905-920.
- King M. A. and Schwinger R. B. (1984). Two dimensional filtering of SPECT images using the Metz & Wiener filters. *Journal of Nuclear Medicine*, **25**: 1234-1240.
- Kramer E. L. and Sanger J. J. (1995). Clinical SPECT imaging, Raven Press Ltd., New York. 52-54.
- Madsen M.T. and Park Ch. H. (1985). Enhancement of SPECT images by fourier filtering the projection image set. *Journal of Nuclear Medicine*, **26**: 395-402.
- Matsunari I., Yoneyama T., Kanayama S., Matsudaira K., Junichi Taki N., Nikolla S.G., Tanomai N., Hisada K. (2001). Phantom studies for estimation of defect size on cardiac <sup>18</sup>F SPECT and PET: Implication for Myocardial Viability Assessment. *Journal of Nuclear Medicine*, **42**: 1579-1585.
- Sankaran S., Frey C., Gilland K. L., Tsui B. (2002). Optimum compensation method and filter cut-off frequency in myocardial SPECT: A human observer study. *Journal of Nuclear Medicine*, **3**: 432-438.
- Van Laere K., Koole M., Lemehieu I., Dielckx R. (2002). Image Filtering in Single Photon Emission Computed Tomography: Principles & Application., *Computerized Medical Imaging and Graphics*, **25**: 127-133.